Reconstruction across imaging modalities: MRI

Brad Sutton

bsutton@Illinois.edu
Bioengineering and Beckman Institute

ILLINOIS
Beckman Institute for Advanced Science & Technology

Introduction to Spins and Classical MRI Physics

Most MRI scans are looking at hydrogen nucleus.

This is good: Body is mostly water ➡ H_2O

Other nuclei are available in MRI:
^{13}C, ^{19}F, ^{23}Na, others

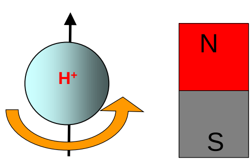

Spinning proton == SPIN
Spinning proton has a magnetic moment ::
Classical Description: Behaves as a bar magnet.

Sample outside the MRI magnet, spins randomly oriented.

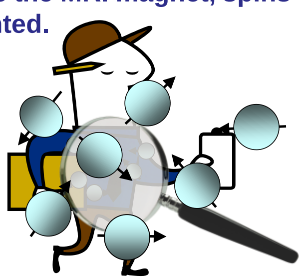

Place sample in the MRI magnet…

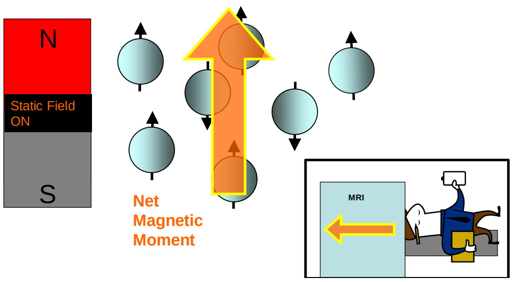

From spins to signal:

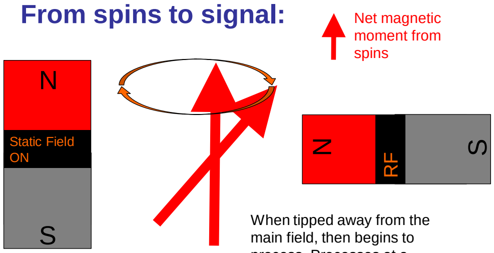

When tipped away from the main field, then begins to precess. Precesses at a frequency proportional to the magnetic field strength. At 3 T = 128 MHz

Localization in Space: Larmor Precession

Since frequency is proportional magnetic field strength if we apply a magnetic field that varies with spatial position, the precession frequency varies with spatial position.

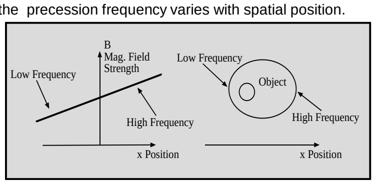

From Noll: fMRI Primer: http://fmri.research.umich.edu/documents/fmri_primer.pdf

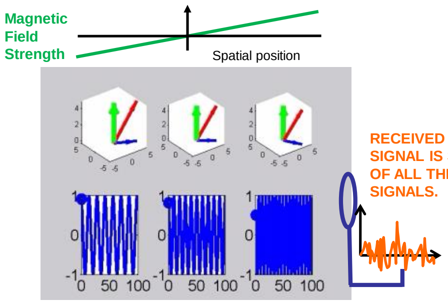

Fourier Image Reconstruction (1D)

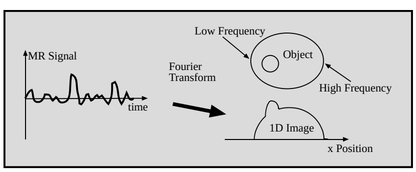

Projection similar to CT!

From Noll: fMRI Primer: http://fmri.research.umich.edu/documents/fmri_primer.pdf

2D Imaging - 2D Fourier Transform

- Fourier encoding also works in 2 and 3 dimensions:

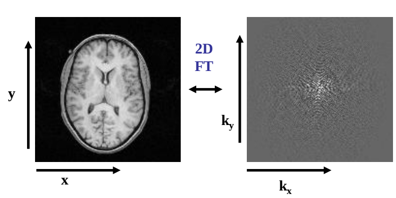

K-space

- We keep track of how much encoding (gradient amplitude times time it is on) by location in k-space:

$$k_x(t) = \bar{\gamma} \int_0^t G_x(\tau) d\tau$$

- This is similar to wave number or K-number, it captures the number of spatial cycles of intensity per unit distance
- Fill in k-space, then reconstruction by Fourier Transform

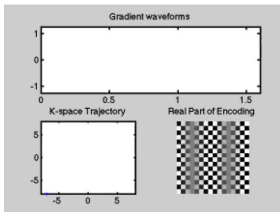

$\bar{\gamma}$ = 42.58 MHz/Tesla

What about non-Cartesian Acquisitions?

- Instead of sampling regular k-space locations on a Cartesian grid, more efficient sampling might include:

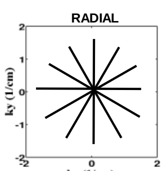

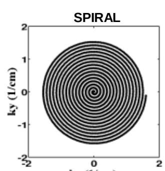

Non-Cartesian: Direct Reconstruction Approach

$$s(\vec{k}) = \int_{FOV} m(\vec{r}) e^{-i2\pi\vec{k}(t)\cdot\vec{r}} d\vec{r}$$

Signal Equation for MRI
NOTE: dr is evenly spaced pixels

- Can perform Inverse Fourier Transform, but must be careful

$$\hat{m}(\vec{r}) = \int_{\vec{k}} s(\vec{k}) e^{i2\pi\vec{k}(t)\cdot\vec{r}} d\vec{k}$$

IFT Reconstruction
NOTE: dk is NOT evenly spaced

- Have to take into account differences in sampling density in different areas of k-space, $d\vec{k}$

Sample Density Compensation

- Density compensation function (DCF) represents the differential area element for each sample.
- Can calculate DCF in many ways:
  – Voronoi area (shown)
  – Analytical formulation of gradient
  – Jacobian of time/k-space transformation
  – PSF optimization

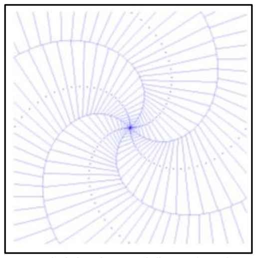

DCF Calculation via Voronoi diagram for 4 shot spiral, showing sampling locations and differential area elements

With DCF, now can perform recon

- Inverse Discrete Space Fourier Transform

$$\hat{m}(\vec{r}) = \sum_j w(\vec{k}_j) s(\vec{k}_j) e^{i2\pi \vec{k}_j \cdot \vec{r}} \qquad w(\vec{k}_j)$$

Density Compensation Function

- But for large problems, we would like to use the Fast Fourier Transform (FFT).
  – **k** is still not equally sampled on regular grid: requirement for FFT!
- What are the options?

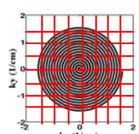

Simply INTERPOLATE onto regular grid and then use FFT?
We will show that we can do better than that with GRIDDING!

Gridding: Fast, accurate, direct recon

- Steps in Gridding
  1. Density compensate k-space data w(**k**)*s(**k**)
  2. Convolution with a fixed-width blurring kernel to fill in continuous sampling of k-space
  3. Resample data at uniform Cartesian locations
  4. Inverse FFT
  5. Deapodization: Eliminate the effect of the fixed kernel interpolator.
     Convolution in k-space is multiplication in image space, so we can remove the effect of the convolution by dividing by the FT of the kernel in image space.

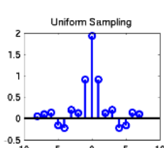

1D simulation from: Noll and Sutton, ISMRM Educational Session, 2003.

Jackson, et al. IEEE Trans Med Imaging. 1991;10(3):473-8.

Gridding is more accurate than interpolation

- 1D Example: Non-uniform spaced samples
- Compared to nearest neighbor interpolation and cubic spline
- Eliminating effect of interpolation drastically increases accuracy!

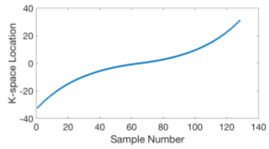

NRMSE:
Nearest: 0.073
Cubic: 0.0143
Gridding: 6.7e-5

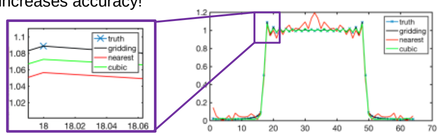

Inverse Problem Approach

Instead of direct inversion, inverse problem approach enables advanced image acquisition and reconstruction

- Variety of additional physics can be accommodated in the signal equation for MRI, enabling advanced acquisitions and reconstructions
  - Coil sensitivities, magnetic field inhomogeneity, k-space trajectory distortions, eddy currents, subject motion, R2* decay, …
- Image regularization penalties can enable faster imaging while making high quality images from fewer samples
  - Total variation, compressed sensing, low rank, …
- Do not need to know sample density compensation function for inverse problem

Signal Model for MRI

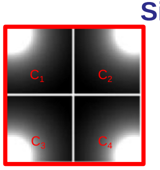

Sensitivity Maps

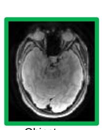
Object

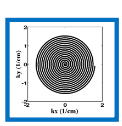

K-space trajectory

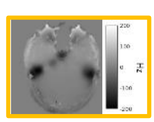

Field Map, ω

$$s_n(\vec{k}_j) = \sum_i \mathrm{sinc}(\vec{k}_j \Delta r) C_n(\vec{r}_i) m(\vec{r}_i) e^{-i2\pi \vec{k}_j \cdot \vec{r}_i} e^{-i\omega(\vec{r}_i) t_j}$$

$$\mathbf{y}_n = \mathbf{s}_n + \epsilon_n = \mathbf{A}\mathbf{C}_n\mathbf{m} + \epsilon_n \quad \Rightarrow \quad \mathbf{y} = \mathcal{A}\mathbf{m} + \epsilon$$

Inverse problem approach

- In complex-valued MRI, noise is complex Gaussian.
- Makes statistics easier than other modalities
- Can use least squares approaches for image reconstruction $\hat{\mathbf{m}} = \arg\min_{\mathbf{m}} \|\mathbf{y} - \mathbf{A}\mathbf{m}\|_2^2$
- Can add regularization to help with the usually ill-conditioned problem, provides prior information on acceptable solutions, through some function $\mathcal{R}()$

$$\hat{\mathbf{m}} = \arg\min_{\mathbf{m}} \|\mathbf{y} - \mathbf{A}\mathbf{m}\|_2^2 + \lambda\mathcal{R}(\mathbf{m})$$

Example: Magnetic Field Inhomogeneity

Incorporation of the field inhomogeneity map into the inverse problem to correct for it.

Air/tissue interfaces cause most magnetic field disruptions, for example around sinuses.

B_0 *(ppm)*

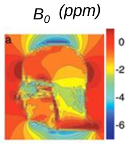

Air/Tissue interfaces can cause up to ~1 KHz off-resonance at 3 T

Image Distortion

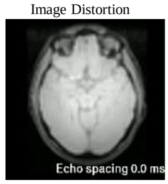

Distortion depends on K-space trajectory and bandwidth (how fast sample k-space).

Example: Magnetic Field Inhomogeneity

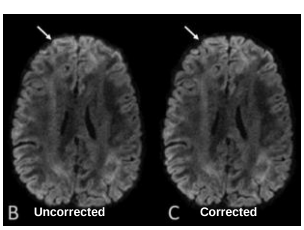

High Resolution (0.8 mm isotropic) diffusion MRI, b=1000 s/mm^2

Dynamic Speech Imaging with FLASH. Air/tissue susceptibility can be 1.2 kHz at 3 T.

Holtrop and Sutton. J Medical imaging. 3(2): 023501 (2016).
Sutton, et al. J Magn Reson Imaging. 32:1228 (2010)

Regularization and Constraints

- Image reconstruction is ill-conditioned problem
  - Sample only the minimum data (or less) that we need to keep scan time short
  - Push the spatial resolution higher → signal-to-noise lower
  - Non-ideal experimental conditions
    - Magnetic field map changed since measurement
    - Coil sensitivies changed
    - K-space trajectory deviations
- Must enforce prior information on the solution in order to achieve a high quality image

Types of Regularization/Constraints in MRI

- Not an exhaustive list, just main ones
- Energy penalty, reference image, Tikhonov
- Roughness penalty, first order derivative,
- TV - total variation
- Compressed sensing
  - Sparsity, Finite differences, DCT, Wavelets, … thresholding

- Something to keep in mind: MRI images are complex valued – have magnitude and phase

Compressed Sensing

- CS takes advantage of k-space sampling patterns that cause **incoherent aliasing** from the undersampling.
  - Distributes aliasing energy around in an incoherent manner
  - Makes it noise-like
- Transforms images into a domain where they are **sparse**
- **Recovers sparse coefficients** in the background noise of aliasing – similar to denoising algorithms

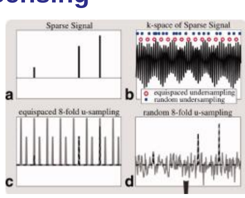

Figure from: Lustig, Donoho, Pauly. Magn Reson Med, 58:1182 (2007)

https://people.eecs.berkeley.edu/~mlustig/CS.html

Low Rank through Partial Separability

- Not only are images typically sparse in finite difference or wavelet domains, dynamic timeseries data are typically low rank
- Low rank indicates strong spatial-temporal correlations in the data set.

- Simple example to play around with at:

http://go.illinois.edu/LowRank

Partial Separability (PS) Model

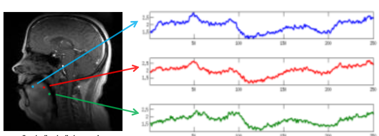

/loo/ - /lee/ - /la/ sounds
100 frames per second

- Leverages strong spatiotemporal correlation
- L^{th} order Partial Separability model:

$$d(\boldsymbol{k},t) = \sum_{l=1}^{L} c_l(\boldsymbol{k})\varphi_l(t)$$

Z.-P. Liang, *IEEE-ISBI,* 2007.

Partial Separability Model

$$s(\mathbf{k},t) = \sum_{l=1}^{L} \underbrace{c_l(\mathbf{k})}_{\text{Spatial Bases}} \underbrace{\phi_l(t)}_{\text{Temporal Bases}} \Rightarrow \mathbf{C} = \begin{bmatrix} s(\mathbf{k}_1,t_1) & s(\mathbf{k}_1,t_2) & \cdots & s(\mathbf{k}_1,t_M) \\ s(\mathbf{k}_2,t_1) & s(\mathbf{k}_2,t_2) & \cdots & s(\mathbf{k}_2,t_M) \\ \vdots & \vdots & & \vdots \\ s(\mathbf{k}_N,t_1) & s(\mathbf{k}_N,t_2) & \cdots & s(\mathbf{k}_N,t_M) \end{bmatrix}$$

$$\text{rank(C)} \leq L, \text{ over any point set } \{(\mathbf{k}_m, t_n)\}_{m,n=1}^{M,N}$$

$$\mathbf{C} = \begin{pmatrix} s(\mathbf{k}_1,t_1) & ? & \cdots & s(\mathbf{k}_1,t_p) & ? & \cdots & ? & s(\mathbf{k}_1,t_m) \\ ? & s(\mathbf{k}_2,t_2) & ? & \cdots ? & s(\mathbf{k}_2,t_q) & \cdots & ? & ? \\ & \cdots & & & & & & \\ s(\mathbf{k}_n,t_1) & ? & ? \cdots & s(\mathbf{k}_n,t_l) & & \cdots & ? & s(\mathbf{k}_n,t_m) \end{pmatrix}$$

$$\hat{\mathbf{C}} = \arg\min_{\mathbf{C}} \| \mathbf{\Pi}(\mathbf{C} - \hat{\mathbf{C}}) \|_2^2 \quad \text{s.t. } \operatorname{rank}(\hat{\mathbf{C}}) = L$$

$$\Downarrow$$

$$\hat{\mathbf{C}} = \arg\min_{\mathbf{C}} \| \mathbf{\Pi}(\mathbf{C} - \hat{\mathbf{C}}) \|_2^2 + \lambda \| \hat{\mathbf{C}} \|_*$$

Z.-P. Liang, *IEEE-ISBI,* 2007.

Partial Separability Model

$$\mathbf{C} = \begin{pmatrix} s(\mathbf{k}_1,t_1) & ? & \cdots & s(\mathbf{k}_1,t_i) & ? & \cdots & ? & \cdots & s(\mathbf{k}_1,t_m) \\ ? & s(\mathbf{k}_2,t_2) & ? & \cdots & ? & s(\mathbf{k}_2,t_j) & \cdots & ? & ? \\ & & \cdots & & & & & & \\ & & \cdots & & & & & & \\ \hat{s}(\mathbf{k}_p,t_1) & \hat{s}(\mathbf{k}_p,t_2) & \cdots & \hat{s}(\mathbf{k}_p,t_i) & \cdots & \hat{s}(\mathbf{k}_p,t_j) & \cdots & \hat{s}(\mathbf{k}_p,t_{m-1}) & \hat{s}(\mathbf{k}_p,t_m) \\ \hat{s}(\mathbf{k}_{p+1},t_1) & \hat{s}(\mathbf{k}_{p+1},t_2) & \cdots & \hat{s}(\mathbf{k}_{p+1},t_i) & \cdots & \hat{s}(\mathbf{k}_{p+1},t_j) & \cdots & \hat{s}(\mathbf{k}_{p+1},t_{m-1}) & \hat{s}(\mathbf{k}_{p+1},t_m) \\ \hat{s}(\mathbf{k}_{p+q},t_1) & \hat{s}(\mathbf{k}_{p+q},t_2) & \cdots & \hat{s}(\mathbf{k}_{p+q},t_i) & \cdots & \hat{s}(\mathbf{k}_{p+q},t_j) & \cdots & \hat{s}(\mathbf{k}_{p+q},t_{m-1}) & \hat{s}(\mathbf{k}_{p+q},t_m) \\ & & \cdots & & & & & & \\ & & \cdots & & & & & & \\ s(\mathbf{k}_n,t_1) & ? & ? & \cdots & \cdots & \cdots & s(\mathbf{k}_n,t_l) & ? & s(\mathbf{k}_n,t_m) \end{pmatrix}$$

Navigator Data

- High temporal sampling speed
- Limited **k**-space locations
- Determines $\{\phi_l(t)\}_{l=1}^{L}$

Imaging Data

- Extended **k**-space locations
- Low temporal sampling speed
- Determines $\{c_l(\mathbf{k})\}_{l=1}^{L}$

28 Z.-P. Liang, *IEEE-ISBI*, 2007.

PS Model-based Image Reconstruction

- **Step 1:** determination of temporal basis functions

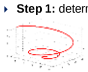

$$\begin{bmatrix} d_1(\boldsymbol{k}_1,t_1) & d_1(\boldsymbol{k}_2,t_1) & \cdots & d_1(\boldsymbol{k}_N,t_1) \\ d_1(\boldsymbol{k}_1,t_2) & d_1(\boldsymbol{k}_2,t_2) & \cdots & d_1(\boldsymbol{k}_N,t_2) \\ \vdots & \vdots & \ddots & \vdots \\ d_1(\boldsymbol{k}_1,t_M) & d_1(\boldsymbol{k}_2,t_M) & \cdots & d_1(\boldsymbol{k}_N,t_M) \end{bmatrix} = \sum_{l=1}^{L} \lambda_l u_l v_l^H$$

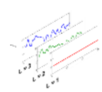

$\{\varphi_l(t)\}_{l=1}^{L}$

- **Step 2:** estimation of spatial basis functions

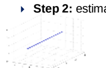

$$\{\hat{c}_l(\boldsymbol{k})\}_{l=1}^{L} = \arg\min_{\{c_l(\boldsymbol{k})\}_{l=1}^{L}} \left\| d_2(\boldsymbol{k},t) - \boldsymbol{E}\left\{\sum_{l=1}^{L} c_l(\boldsymbol{k})\varphi_l(t)\right\}\right\|_2^2$$

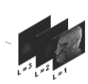

$\{C_l(\boldsymbol{r})\}_{l=1}^{L}$

- **Step 3:** synthesis of (***k***, *t*)-space / (***x***, *t*)-space data

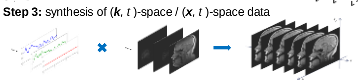

Fu et al, Magn Reson Med, 2015, 2017

PS-Sparse Reconstruction

- Jointly enforcing the partial separability constraint and the spatial-spectral sparsity constraint

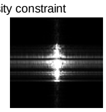

(*x, f*) - spectrum

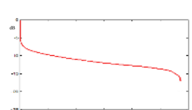

Sorted (*x, f*) - coefficients

- Formulation: $$\{\hat{c}_l(\boldsymbol{k})\}_{l=1}^{L} = \arg\min_{\{c_l(\boldsymbol{k})\}_{l=1}^{L}} \underbrace{\left\| d_2(\boldsymbol{k},t) - \boldsymbol{E}\left\{\sum_{l=1}^{L} c_l(\boldsymbol{k})\varphi_l(t)\right\}\right\|_2^2}_{\text{Data consistency constraint}} + \lambda \underbrace{\left\| \boldsymbol{F}_{k,t}\left\{\sum_{l=1}^{L} c_l(\boldsymbol{k})\varphi_l(t)\right\}\right\|_1}_{\text{Spatial-spectral sparsity constraint}}$$
- An algorithm based on half-quadratic regularization has been proposed to solve this optimization problem [1].

[1] B. Zhao *et al*, *TMI,* 2012.

What you can achieve with PS-Sparse

Subject:
A female speaker of Mid-Atlantic American English
Spatial coverage:
$280 \times 280 \times 40$ mm^3
Matrix size:
$128 \times 128 \times 8$
Spatial resolution:
$2.2 \times 2.2 \times 5.0$ mm^3
Nominal Frame Rate:
166 frames per second!

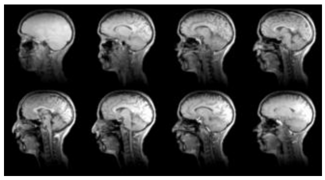

Carrier Phrase – "I said writing to you, I said riding to you" [1]

Fu, Barlaz, Holtrop, et al. Magn Reson Med 77(4): 1619, 2017. M. Barlaz et al, InterSpeech, 2015.

Speeding Up Acquisitions: Parallel Imaging

- Reconstruction approaches above did not leverage the use of multiple, smaller receiver coils
- Each coil is most sensitive to tissue in its local area
- Reduced spatial encoding requirements because aliasing signal may overlap region where there is low sensitivity for a coil
- Easily incorporated into cost function for sensitivity encoding (SENSE)

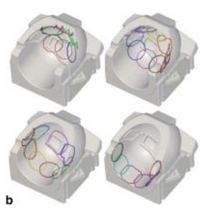

Kaza, Klose, and Lotze. J Magn Reson Imaging. 34:173 (2011)

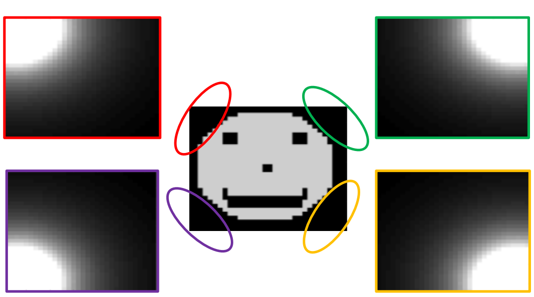

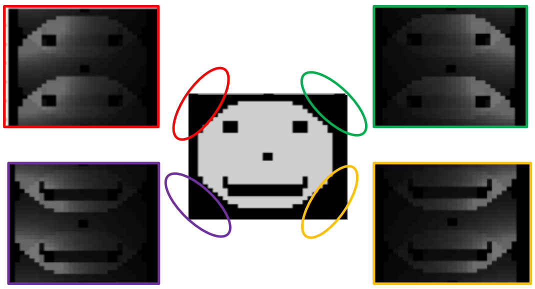

Parallel Imaging Reconstruction

- SENSE – least squares estimation with coil sensitivities in image space

$$s_n(\vec{k}_j) = \sum_i \mathrm{sinc}(\vec{k}_j \Delta r) C_n(\vec{r}_i) m(\vec{r}_i) e^{-i2\pi \vec{k}_j \cdot \vec{r}_i} e^{-i\omega(\vec{r}_i)t_j}$$

- GRAPPA – operates in k-space. Multiplication by coil sensitivities in image space is convolution in k-space. So, find the convolution kernel in k-space to fill in missing samples

Pruessmann, et al. Magn reson Med 42:952 (1999). Griswold, et al. Magn Reson Med 47: 1202 (2002)

GeneRalized Autocalibrating Partially Parallel Acquisitions (GRAPPA)

- Learn linear relationship between kernels of sampled points in k-space to "interpolate" those that were not sampled.

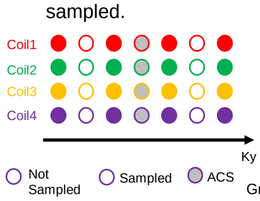

Griswold, et al. Magn Reson Med 47: 1202 (2002)

GeneRalized Autocalibrating Partially Parallel Acquisitions (GRAPPA)

- Learn linear relationship between kernels of sampled points in k-space to "interpolate" those that were not sampled.

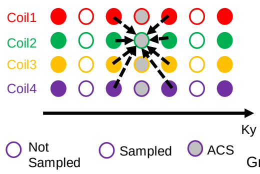

Using Autocalibration points, find the weights required to fit the target point, using adjacent samples from across all coils.

Griswold, et al. Magn Reson Med 47: 1202 (2002)

GeneRalized Autocalibrating Partially Parallel Acquisitions (GRAPPA)

- Learn linear relationship between kernels of sampled points in k-space to "interpolate" those that were not sampled.

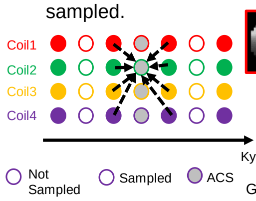

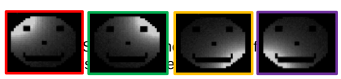

Once k-space filled in – simply Fourier Transform to make an image from EACH COIL.

Griswold, et al. Magn Reson Med 47: 1202 (2002)

COMPUTATIONAL Challenge of Image Reconstruction

- Large matrix size
  - 1.25 mm isotropic data set
- Data Size:
  - 18 GB for 6.5 min scan
- Physics:
  - 3D non-Cartesian (Spiral) sampling
  - Parallel Imaging with 32 channel coil
  - Magnetic Field Inhomogeneity Correction
  - Motion-induced Phase Correction
- Reconstruction Time
  - 8 days for reconstruction running on workstation
- Graphics Processing Units (GPU)
  - 200 times faster: <1 hour.
  - Enables imaging resolutions not feasible before.

GTX 1080 Ti: ~$700 (11 GB)
CORES: 3584
Boost Clock: 1582 MHz

IMPATIENT MRI:
Illinois Massively Parallel Acceleration Toolkit for Image reconstruction with ENhanced Throughput in MRI

PowerGrid –ISMRM 2016, p. 525

PowerGrid: A open source library for accelerated iterative magnetic resonance image reconstruction

Alex Cerjanic[1,2], Joseph L Holtrop[1,2], Giang Chau Ngo[1], Brent Leback[3], Galen Arnold[4], Mark Van Moer[4], Genevieve LaBelle[2,5], Jeffrey A Fessler[6], and Bradley P Sutton[1,2]

ISMRM 2016, p. 525

http://mrfil.github.io/PowerGrid/

- Enable leveraging of GPU and MPI in MRI reconstructions
- Using ISMRM RD – raw data format standard
- Translating MATLAB routines from IRT into C++ through Armadillo
- Packaging for easy use (Docker) – coming soon

Scale with PowerGrid

- How to use > 1 GPU?
- Message Passing Interface (MPI)
- Phase Corrected SENSE (pcSENSE) for Diffusion Imaging
  - 120 x 120 x 4 x 32 coils

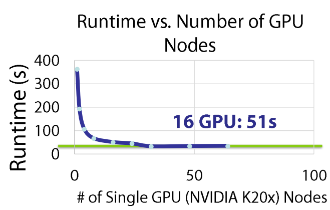

Liu C, Moseley ME, Bammer R. Simultaneous phase correction and SENSE reconstruction for navigated multi-shot DWI with non-cartesian k-space sampling. MRM. 2005;54(6):1412–1422.

K20x: 2688 cores, 732 MHz clock rate. 6 GB.

Push for Free, Open Source, Common Platforms for Image Reconstruction

- Advanced reconstructions are more complex than Fourier Transform, but enable significantly higher resolutions and shorter scan times.
- Image reconstructions can be specific for the sequence, MRI vendor platform, image reconstruction hardware, and can be difficult to reimplement from paper
- There is a growing effort at creating broad-based utilities to enable reproducibility, distribution, scaling, and impact
- Just a few listed here…

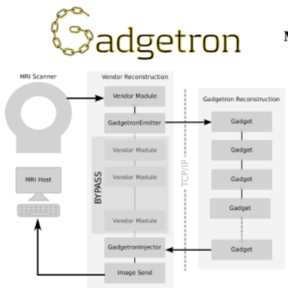

Hansen and Sorensen. Gadgetron. Magn Reson Medicine 69: 1768 (2013)

Michigan Image Reconstruction Toolbox (MIRT)
https://web.eecs.umich.edu/~fessler/code/index.html

https://www.ismrm.org/MR-Hub/

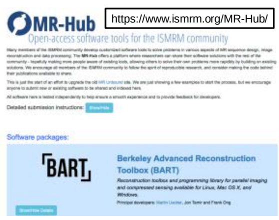

Summary

- Inverse problem approach to MRI reconstruction enables higher resolution, improved SNR, accommodating non-ideal physics for improved image quality
- Comes at a great deal of computational expense (MRI scanner does an efficient job for FFT on Cartesian data)
- Lots of open source powerful code available to translate techniques to clinical research workflows, leveraging clusters and GPU's
  – TRY THEM OUT!